

Development of a High Torque Density, Flexible, Composite Driveshaft

Duncan J. Lawrie
President
Lawrie Technology, Inc.
Girard, Pennsylvania
duncan@lawrietechnology.com

Abstract

An all-composite driveshaft incorporating integral flexible diaphragms is described. An approach was explored which obsoletes the split lines and associated fasteners required to attach metallic flex elements and either metallic or composite spacing tubes in current solutions. Sub-critical driveshaft weights half that of incumbent technology are projected for typical rotary wing shaft lengths. A description of the trade-off required between axial, bending, and torsional stiffness plus torque density and manufacturability is provided. Fully anisotropic material properties were mapped to the deeply sculpted diaphragm geometry and a parametric, numerical study of the complex shell undertaken. Spacing tubes are described, which comprise an integral part of the initial tooling but which remain part of the finished shaft and control natural frequencies and torsional stability. A concurrently engineered manufacturing process and design for performance is described which competes with incumbent metal solutions at lower weight and with the probability of improved damage tolerance and fatigue life

Introduction

This research addresses rotary wing power transmission in the area of flexible driveshafts. These are crucially important components for conventional helicopters at engine to gearbox, tail-rotor drive, and main mast locations. In the case of tilt-rotors the cross-over wing driveshafts rely extensively on the technology. Typically, titanium, aluminum or composite shafts are bolted through curvic face connectors to titanium diaphragm couplings to accommodate airframe distortions while transmitting the requisite power. These flexible drive trains emphasize minimum weight and hence demand torque density and small size. In the case of drive trains passing through flexing wing and fuselage structures the need for motion accommodation is also greater than for ground-based equipment – typically between 1.0 and 2.0 degrees per end. Power transmission coupling elements, which accommodate axial, bending, and transverse displacements, must do so while simultaneously carrying relatively large torsional loads. In short, it is difficult for a structural metallic membrane to simultaneously carry very large torsional shear and remain conveniently compliant to imposed out-of-axis distortions. Figure 1 depicts an assembly using four membrane type flexible metallic diaphragms at each end of a spacing shaft. Aircraft use, particularly rotary wing, more typically demands high angular motion to follow structural deformations. One expedient used to minimize weight is to operate at very high rotational speed such that torque is minimized for a given power. Limiting this high rpm is dynamic instability or classical “whirling”. Additional instabilities that affect the spacer shaft also include axial or “hunting” motions and torsional oscillations. Variables that drive

this behavior are mass per unit length, axial, bending, and torsional stiffnesses - and boundary conditions. Clearly the primary objective for drive trains such as these is to allow bending rotations at each end, thus prescribing the boundary conditions. This, then, reduces the speed at which the fundamental bending or whirling speed is encountered. State-of-the-art helicopter transmissions are operated below this critical speed in order to avoid the large lateral excursions that occur and the associated risk to the shaft plus adjacent wiring harnesses and hydraulic lines. A large literature exists concerning math modeling of this kind of dynamic behavior. However, axial force, large applied torques, shear forces and end moments all affect the prediction of natural frequencies. Much of the literature decouples the effects of some or all of the applied loading to reduce the complexity of the problem. For this reason natural frequencies are most often determined experimentally. Modern composite materials add greatly to functionality and design freedom but anisotropic material properties further complicate the analyses.

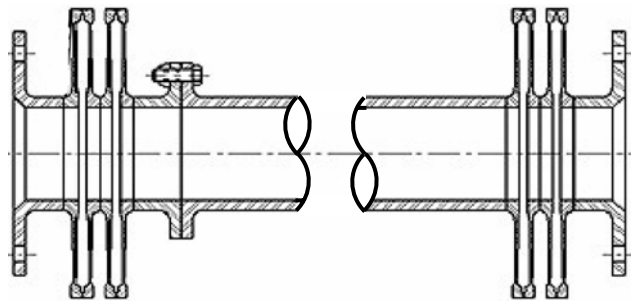


Figure 1 Conventional flexible metallic coupling assembly

The work presented in this paper has concentrated on 6-inch diameter flexible composite coupling elements and integral spacing tubes. This size is typical of tilt-rotor usage and larger conventional tail rotor drives. Figure 2 shows an in-process element with two bolted split lines exactly as for the incumbent titanium technology. This approach used carbon and glass fiber derivatives filament wound into very short hyperbolic geometries such that the outside diameter exhibited fiber angles of approximately 45 degrees and the inside diameter angles were approximately 80 degrees. For this reason, the effective shell stiffness tangentially is higher than it is radially and more angular motion should be possible. A further advantage is the geodesic winding path that facilitates manufacture but also eliminates all stresses other than fiber direction stresses, for thin membranes, when torque and motions are imposed. Limiting aspects of the concept include the thickness build-up where the fiber angle is steepest at the inside diameter. This detail requires that the diaphragms remain thin-walled and effectively limits the maximum torque that can be carried. Nevertheless, torque density and angular motion are comparable with metallic membranes. Perhaps most



Figure 2 S2-glass flex element being wound

significantly the outstanding fatigue performance of unidirectional composites is manifested here because all loading actions give rise to differential tension and compression in the fiber direction and shear stresses tend to zero when the wall thickness is small. Unlike metal diaphragms this is also projected to allow significant damage to be present without catastrophic consequences because – without in-plane shear – each of hundreds of individual fiber bundles comprising the diaphragms behave exactly like a large number of redundant load paths.

The coupling element of figure 2 has been studied extensively in a six-inch envelope and analytical scaling laws developed. Prior composite couplings and integrated driveshaft developments include braided solutions¹; elastomeric matrix composites (under the writer’s direction); and numerous filament wound and pressed diaphragms, link packs, shim packs and similar. Without exception these

research programs provided attractive bending motion and reduced weight but gave up torque density to the extent that they are not fielded solutions today. Most commonly, torque capacities consistently fell short of expectations because the fiber architecture always included local bending in the braid or wind. Also, the prescribed geometry typically required that the composite laminate be “pushed” into shape before curing. The beam-column behavior of compression fibers in the first instance and developed shear stresses due to bending in the second conspired to give up nearly 90% of the achievable torque in every case. Elastomeric matrix composites have frequently been proposed as materials suitable for flexible driveshafts because of the obvious out-of-plane compliance possible. Unfortunately, the compression component of in-plane shear due to torque suffers from low micro-buckling strength and quite low torque density results. For a given fiber volume fraction in a composite shell the compression strength is linearly proportional to the shear modulus of the matrix resin. Suitable elastomeric resins provide shear moduli from 1 – 10% of that obtained using a typical epoxy. Further, all available elastomeric systems tend to produce limiting hysteretic heating effects under imposed bending motions.

This research has finessed both the design for performance and the manufacturing process using epoxy resins such that sustainable compression components of composite stress under pure torque are now approaching 170 ksi. This is achieved via a hands-off CNC controlled, repeatable process using traceable pre-impregnated materials and the approach also avoids bolted split lines and large fastener count. In the case of tilt rotor wing cross-over drives the weight savings are projected to be approximately 55%. Additionally, the avoidance of split line fasteners is projected to reduce windage losses and associated heat and noise generation substantially.

Testing Experience:

Full load dynamic testing using closed loop simulation rigs has been undertaken on early prototype flexible shafts as shown in figures 3 and 4.



Figure 3 Early prototype flexible composite shaft

Test Block	Angular displacement	Torque [Nm]	Torque [in.lb]	Total of cycles	
#1	1.0 deg	565 Nm	5 000	500 000	PASSED
#2	1.0 deg	1130 Nm	10 000	500 000	PASSED
#3	1.0 deg	1412 Nm	12 500	500 000	PASSED
#4	1.0 deg	1920 Nm	17 000	500 000	PASSED
#5	1.5 deg	565 Nm	5 000	500 000	PASSED
#6	1.5 deg	1130 Nm	10 000	500 000	PASSED
#7	1.5 deg	1412 Nm	12 500	500 000	PASSED
#8	1.5 deg	1920 Nm	17 000	500 000	PASSED
#9	2.0 deg	565 Nm	5 000	500 000	PASSED
#10	2.0 deg	1130 Nm	10 000	500 000	PASSED
#11	2.0 deg	1412 Nm	12 500	500 000	PASSED
#12	2.0 deg	1920 Nm	17 000	500 000	PASSED

Test	#1	#2	#3	#4	#5	#6	#7	#8	#9	#10	#11	#12
speed	[rpm]	[rpm]	[rpm]	[rpm]	[rpm]	[rpm]	[rpm]	[rpm]	[rpm]	[rpm]	[rpm]	[rpm]
	6700	6700	6700	4500	6000	5000	5000	4000	4500	4500	4000	3500
	-	-	5000	-	-	-	4000	-	-	-	-	-
Total: 500,000 cycles	✓	✓	✓	✓	✓	✓	✓	✓	✓	✓	✓	✓

Figure 4 Closed loop test results

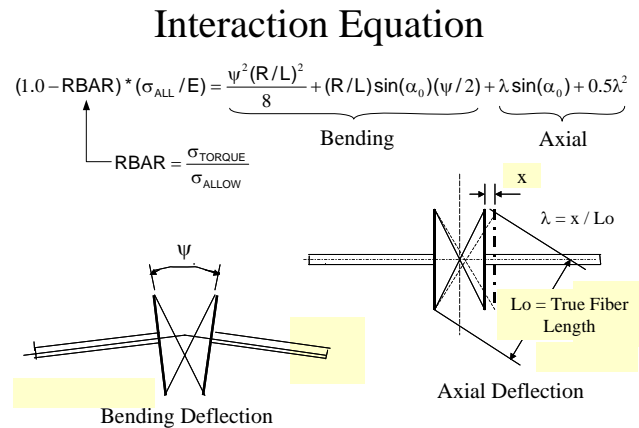
These first results incorporating axial and bending motions plus torque were encouraging. When repeated in a different location using the same load spectrum a problem was found. While no loss of torque capacity or torsional stiffness was experienced, the use of on-board accelerometers highlighted a reduction in axial natural frequency that was eventually attributed to delamination in the diaphragm region. It is likely that this behavior was also manifested in the prior test but not identified.

Hence, this early testing produced a non-catastrophic change in axial stiffness as the variable thickness diaphragms transitioned into a shim pack without loss of load. Clearly the issue must be resolved by removing or by reducing the bending shear stresses. Analytical math models (stick models) capture most stiffness and performance parameters accurately but as more thickness is added to increase torque the contributions of geometry to axial and bending stiffness reduce the accuracy.

Continuing development of coupling elements (without spacing tubes) focused upon hyperbolic geometries offering acceptable torque and minimum shell bending stress without reducing thickness so much that torsional buckling of the diaphragm occurred before the in-plane strength was reached. With two degrees of bending per shaft end targeted a single hyperbolic flex element was required to provide ½ degree per end. In no case was hysteretic heating experienced but it was clear that when thickness was increased above that required for ~60,000 in.lb torque in a 6_inch diameter then ½ degree per diaphragm resulted in delamination over time. All comparison tests included axial and bending stiffness measurement, spin testing up to ½ degree bending per diaphragm (1 degree per flex element) and 7,500 rpm, followed by static torque to failure. Repeat axial stiffness tests were conducted after each increasing angular misalignment on the spin rig in an effort to pinpoint the onset of through-thickness shear failure.

Performing the necessary sensitivity study to compare with this increasing database of test results and to find the available design space now required numerical modeling. The deeply sculpted diaphragms were an integral part of a single continuously wound anisotropic shell created on a perfect geodesic path. The diaphragm regions were comprised of constantly varying thickness and constantly varying material properties. This combination in a fully parametric FEA model was far from trivial.

Main Body



Coupling Performance Envelope

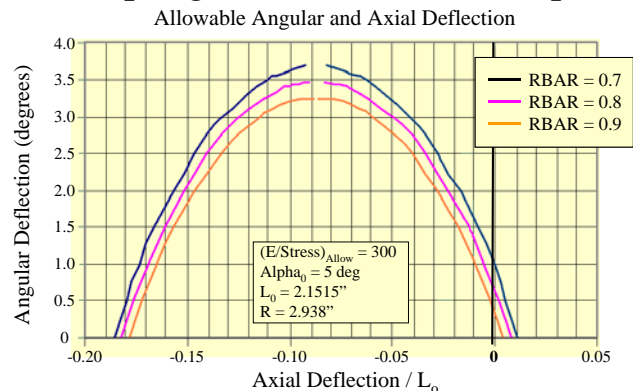


Figure 5 Analytical Design Space (No thickness effects)

The expression provided in figure 5 includes strain components due to axial and bending imposed motions. The LHS of the expression provides for the residual strain available to carry torque assuming a material design allowable. Clearly this approach is accurate assuming no thickness effects, and any desirable combination of imposed motion and torque consume the available design strain. The expression is also that of an ellipse and the non-dimensional

elliptical design space is shown where alpha is the helix angle made by the fiber at the inside diameter to the diametral plane. Given that compressively loaded fibers fail before tensile fibers in the shell and that only fiber direction tension and compression exists for small thickness (when wound on a perfect geodesic) then greater torque and higher bending should be achievable when axial shortening is avoided and shafts are initially installed with small axial tension. The left upper quadrant of the elliptical design space depicted is considered to represent the strain space following snap-through buckling of the diaphragms. Because associated shock loading is undesirable in dynamic shaft applications this large additional design space is, regrettably, unavailable although the steadily reducing stiffness as snap-through is approached might be useful. Couplings with <10,000 in.lb torque to failure and small thickness were produced which exhibited this behavior and provided for >5 degree angular misalignment and >0.3 inch axial motion per diaphragm pair. When 20% more thickness was incorporated, the torque to failure increased by 150% and, indeed, the failure mode was demonstrably one of torsional buckling in the diaphragms. With diminishing progress in the effort to bring analytical models closer to the precisely manufactured test articles the continuing research inevitably required sophisticated parametric FEA models to further understand the available design space. Further study of snap-through buckling was not continued because in fully integral or even assembled driveshafts at least one pair of diaphragms per end is required. Inevitably this means that one diaphragm will attract all the motion because of the unstable stiffness response.

In the figure 5 schematic showing angular misalignment (ψ) the straight generation lines used to represent two hyperbolic fiber paths do not cross on the centerline – unlike that shown for axial displacement. It is useful to visualize a bundle of straws or pencils bound mid-length and then twisted about the axis to produce a hyperbola when viewed laterally. In the case of the composite flex element an open inside diameter exists such that the inside radius provides the torque arm necessary for each fiber bundle to contribute to power transmission (see figure 6).

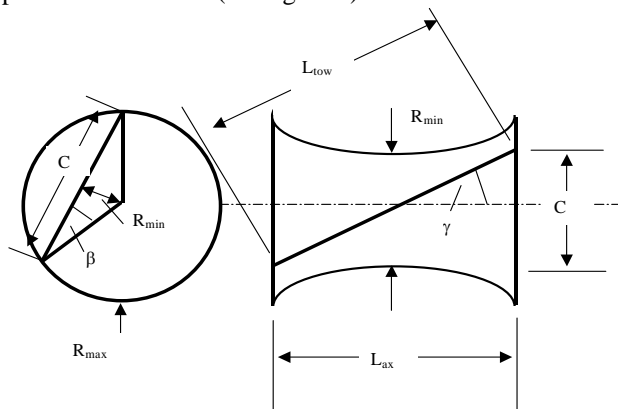


Figure 6 Analytical model basis

In resolving fiber strains a family of trigonometric relations were developed and simply scaled by the number of fiber passes used to provide axial, bending and torsional stiffness values plus anticipated strength limits. It is not useful to reproduce these here. Steel and titanium flanges were analyzed via finite element modeling and the respective

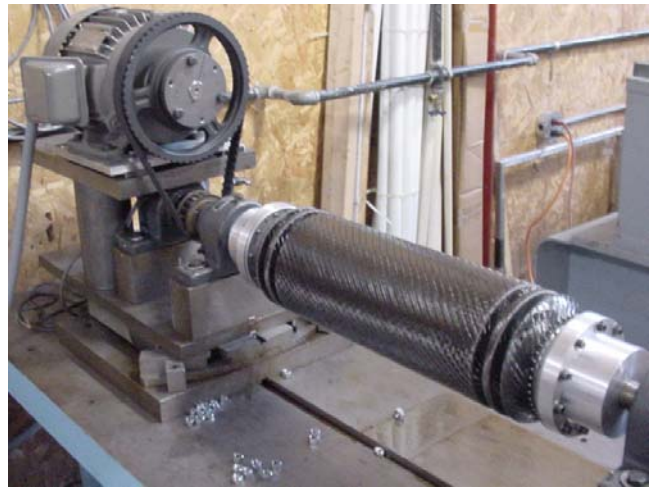


Figure 7 Spin test with bending

flange stiffnesses subtracted as springs in series from test results for the purpose of comparing composite performance with the analytical models. The lack of bending symmetry in the above referenced schematic (figure 5) created concerns as to fidelity of motion in a misaligned, rotating, shaft thus constructed. In fact, very smooth operation was always observed and the precisely controlled manufacturing process even produced shafts that did not require subsequent balancing. In summary, the inability to closely match bending and axial stiffness predictions and the non-existence of lateral oscillations under imposed bending points toward diaphragm bending stress development not predicted by the analytical models. Torsional performance remains accurately predicted however. In figure 7 an all carbon fiber shaft is shown in the spin rig with 2 degrees of imposed bending at each end. Later prototypes used S2-glass fiber exclusively to carry torque with carbon fiber sandwiching this material in the spacing tube such that shaft stability, inertia, and natural frequencies could all be optimized. (See figure 9).

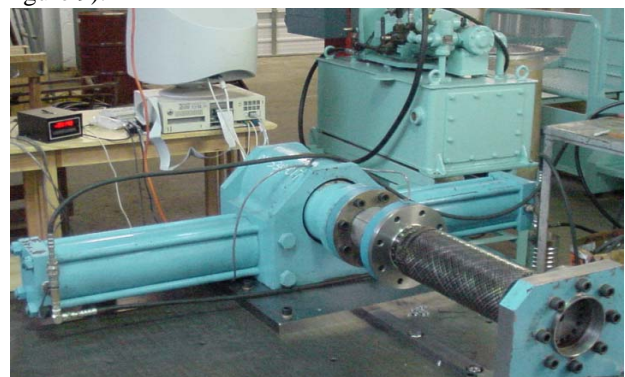


Figure 8 Static Torque rig

The use of S2-glass fiber provided for three times the strain to failure of standard modulus carbon fiber without giving up load density. All prototype shafts have been built with spacing tube diameters equal to the outside diameter of the integral flex element. This is primarily because, for suitably compliant hyperbolic geometries, the fiber angle exiting the diaphragm is typically 42 – 48 degrees. In the paradigm shift that is an integral all-composite flexible shaft it makes no sense to reduce the diameter of the spacing tube because tube wall thickness would have to increase as the fiber angle also increased and shear strength reduced. While this trade-off is at zero weight change, tooling would be adversely affected, as would torsional buckling performance at reduced tube diameters. With (0/90) carbon content in the tube dedicated to achieving torsional stability and tuning natural frequencies, the S2-glass fiber (+/-45) obviously allows for increased torsional wind-up in long shafts. While the lower modulus is desirable in the compliant, integral flex elements the spacing tube serendipitously compensates via the larger than traditional tube diameter.



Figure 9 Hybrid S-2 glass shaft at 7,500 rpm and 2 deg.

Finite Element Modeling

An ANSYS parametric FEA file was written allowing for variable hyperbolic geometry including length, inside diameter, outside diameter, outer composite thickness and boundary conditions. The metallic flange attachments were represented by springs and PLANE25 harmonic axisymmetric elements were used to keep the run time low while still allowing fully orthotropic material properties and non-axisymmetric loads (bending). Meshing strategy maintained 10 elements through the thickness and acceptable aspect ratios regardless of hyperbolic geometry. Prior analytical models accurately provided for membrane fiber direction stresses so the primary objective of the numerical model was to quantify diaphragm bending stresses and determine the critical locations. The fiber crossing angle changes rapidly with radial position, as does the developed composite thickness. Because composite shell elements were not deemed suitable for our present purpose, only the element I_J side was practical for a material coordinate system. All nine independent stiffness terms were mapped as a function of θ and curve fitted with the resulting expressions used to generate 78 discrete material property cards.

Three sequential load steps were used to apply 10,000 in.lb torque; 100 lb axial compression; and 100 in.lb bending. By interrogating the as-calculated solution, meridional (I_J side) stresses were plotted as well as hoop (circumferential) and in-plane shear stresses due to torque. It should be noted that these reported stress results are not fiber direction stresses but require further transformation should this be required. For the present purpose the comparative behavior is of most interest.

After completion of the axisymmetric sensitivity study the model was further developed to produce a full 3_D mesh suitable for extracting eigenvalue buckling solutions under applied torque. In this fashion the design space possible between thin, unstable diaphragms and those too thick to sustain required bending motions was sought out.

Results: Two different hyperbolic geometries are presented graphically to show significant findings. While all results presented use a 6_inch outside diameter the inside diameter was varied from 3.75_inch to 4.9_inch and outer thickness varied from 0.018_inch to 0.03_inch. Immediately obvious was that all meridional stress maximums occurred in the middle of the diaphragm whether caused by axial or bending loads. Conversely, all hoop stress maximums occurred at the outer extremity as did in-plane shear stress due to applied torque. This was true regardless of hyperbolic geometry although peak values obviously varied.

Also clear is the different thickness distribution developed by the deeper cross-section with small outer thickness versus the shallower profile with larger outer thickness. In the latter case the torque capacity is substantially higher and the developed bending stresses much lower. It is perhaps worth pointing out here that, regardless of the technology used,

flexible driveshafts sustain essentially steady state stresses due to both applied torque and imposed axial motion but high frequency cyclic loading due to imposed angular misalignment. For this reason the magnitude of bending stresses are of particular interest. Less intuitive is the fact that the bending stiffness of the shallower diaphragm pair in

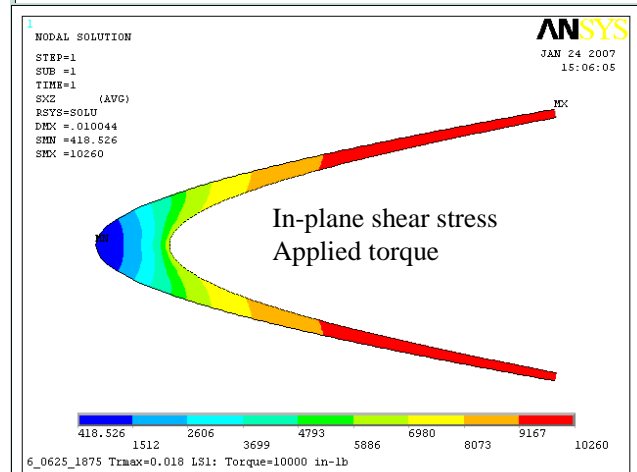
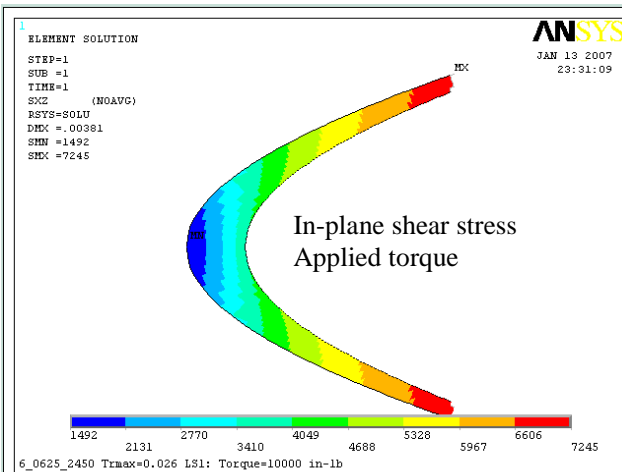
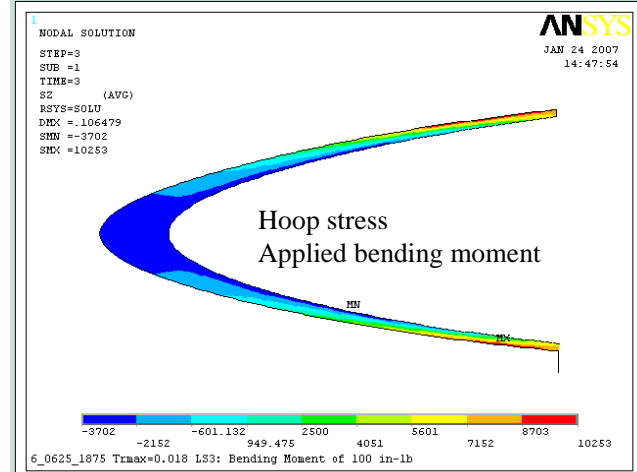
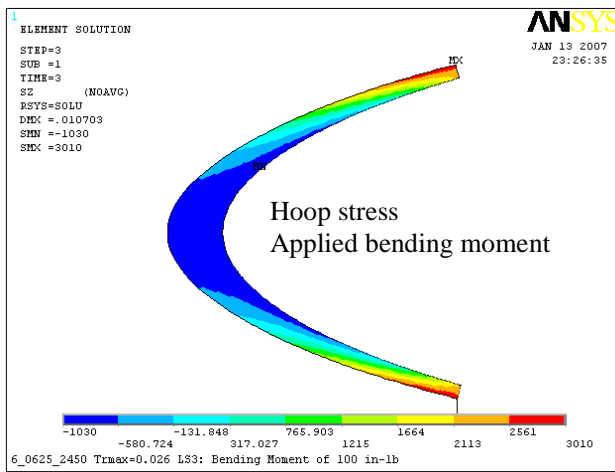
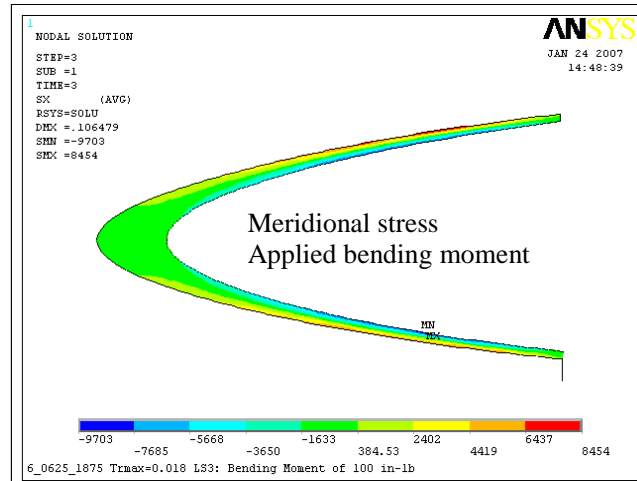
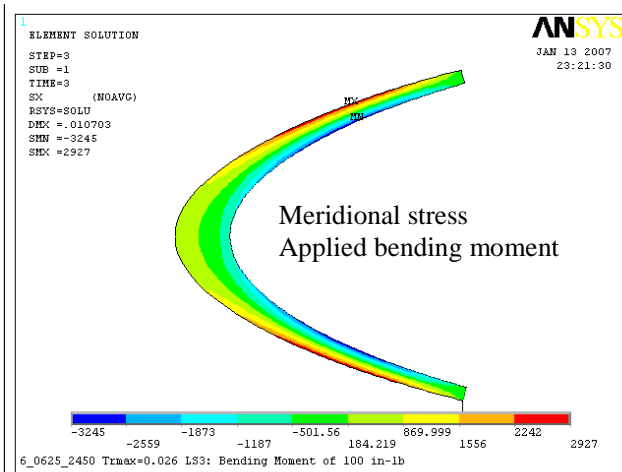


Figure 10 4.9_inch ID/0.026_inch outer thickness

Figure 11 3.75_inch ID/0.018_inch outer thickness

figure 10 is 993 in.lb/deg while the deeper diaphragm of figure 11 is less than 250 in.lb/deg. So while the skinnier profile sustains three times the meridional stress of the thicker profile under 100 in.lb bending moment the actual applied bending moment will only be one quarter because structural deflections are applied in service rather than bending moments. Review of axial loading in figures 12 and 13 clearly demonstrate the benefits of installed axial tension to offset both peak hoop and meridional stresses sustained under angular misalignment. While the skinnier geometry of figures 11 and 13 appears to have a slight advantage in sustaining motion with lower bending stress there remains the issue of torsional buckling of thinner, deeper diaphragms. Figure 14 plots the meridional stress due to diaphragm bending against inside diameter and outer composite thickness and it would appear as though a much smaller penalty exists for adding thickness to deeper diaphragms than to shallower ones. Figure 15 plots the torque reaction of the geometries studied following 1/2 degree of torsional wind-up. Superimposed on these are eigenvalue buckling solutions suggesting minimum outer thickness of 0.025_inch for a 4.0_inch ID and 0.02_inch for a 4.9_inch ID.

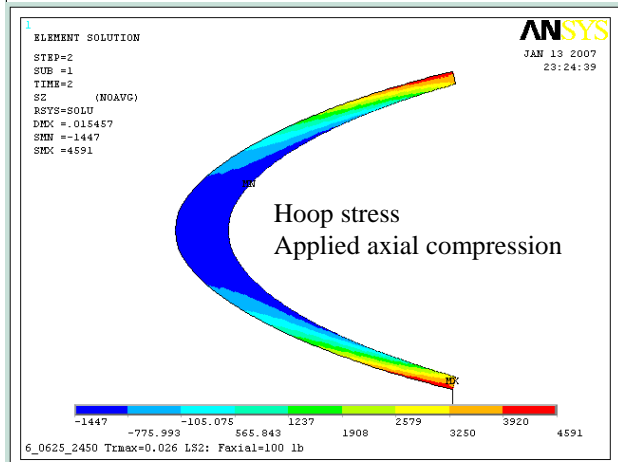
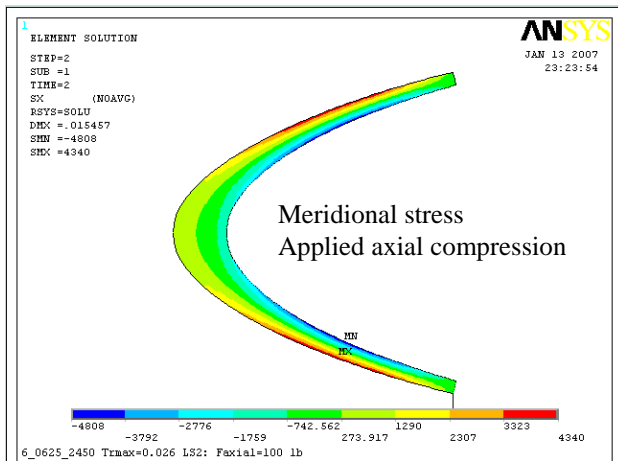


Figure 12 4.9_inch ID/0.026_inch outer thickness

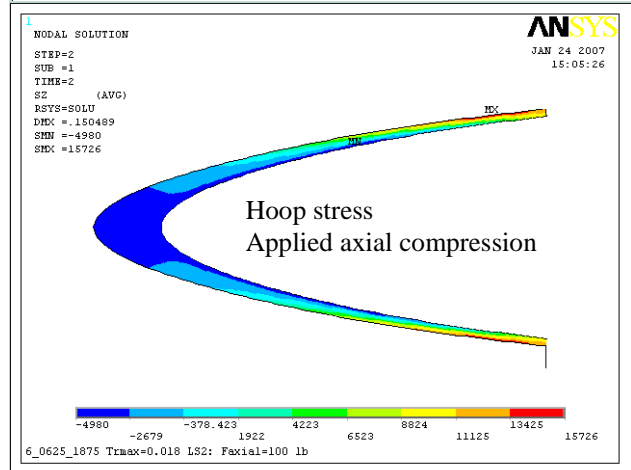
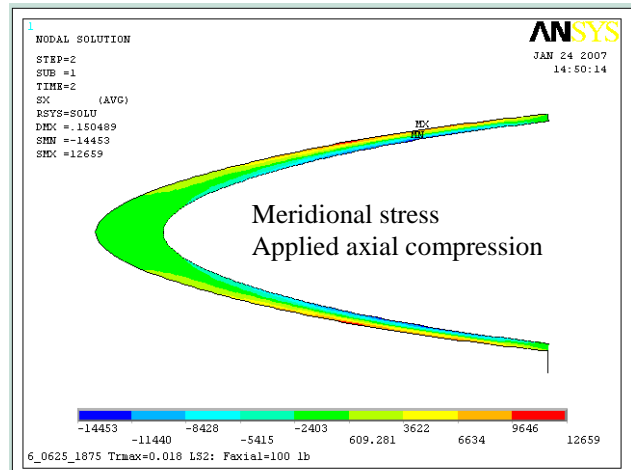


Figure 13 3.75_inch ID/0.018_inch outer thickness

Figure 16 provides a survey of design parameters for all-composite integral flexible shafts produced using the techniques described in this paper. All-inclusive shaft weights are plotted using steel flanges optimized for infinite fatigue life. These weights should be reduced by 2.7 lb per 8_inch shaft and 1.6 lb per 6_inch shaft when using titanium. Fundamental flexural resonance is calculated using spacing tubes which comprise 90 degree (hoop) carbon fiber both inside and outside of the +/-45 degree continuous S2-glass. In the event that higher sub-critical speeds are required then some fraction of the 0.04_inch thick (total) carbon hoop material may be replaced by 0 degree plies. In this way longitudinal modulus increases without a change in shaft weight being incurred.

Figure 14 Diaphragm Bending Stress for a Family of 6_Inch Diameter Hyperbolic Coupling Geometries Subjected to 1/2 degree Angular Misalignment

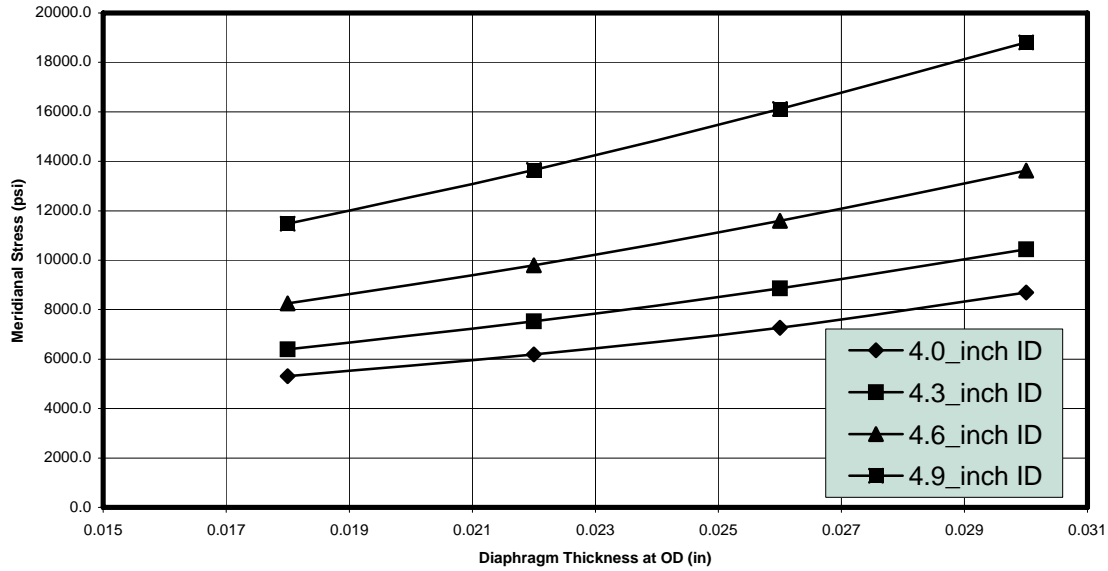
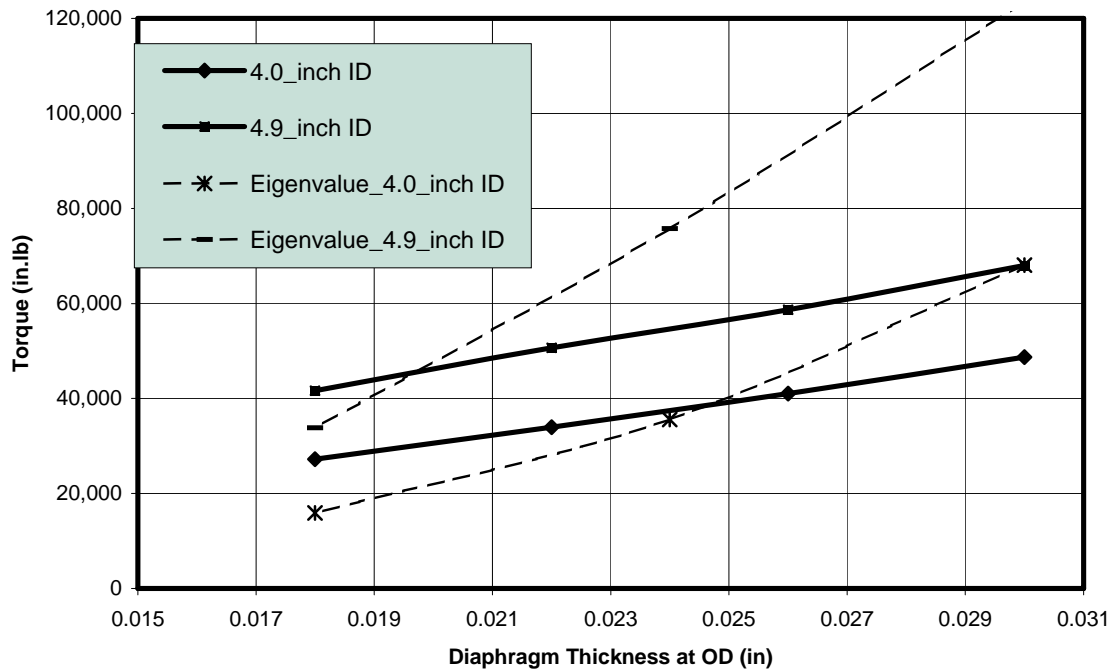
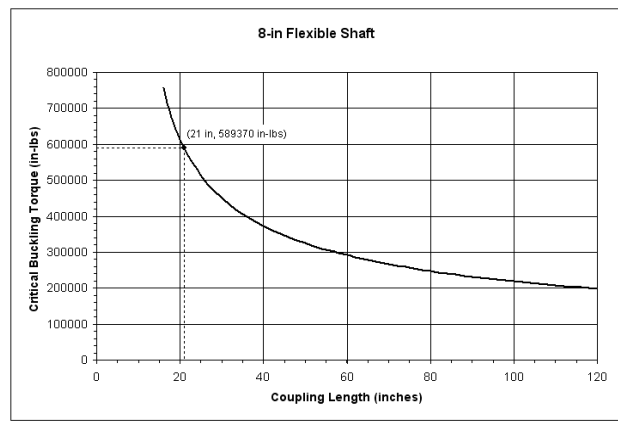
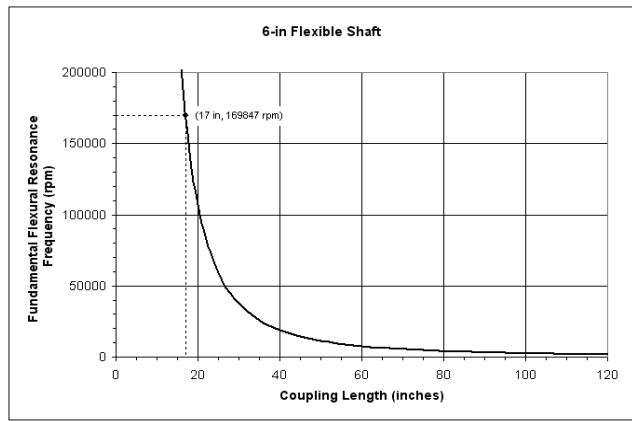
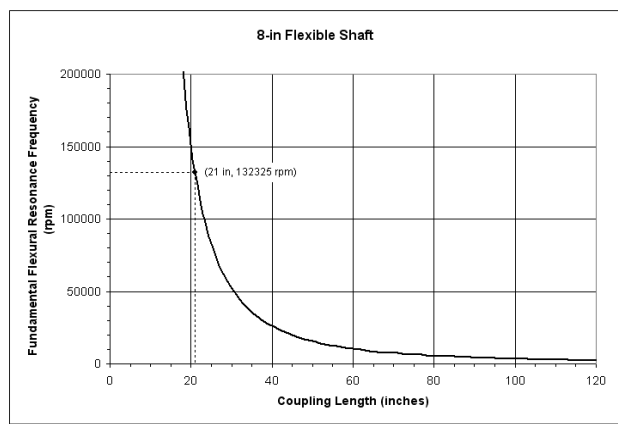
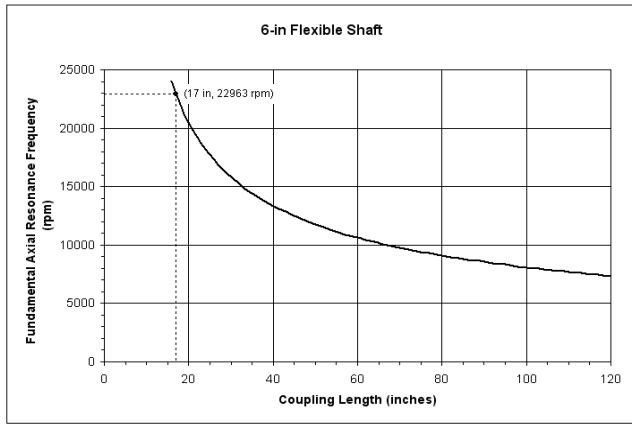
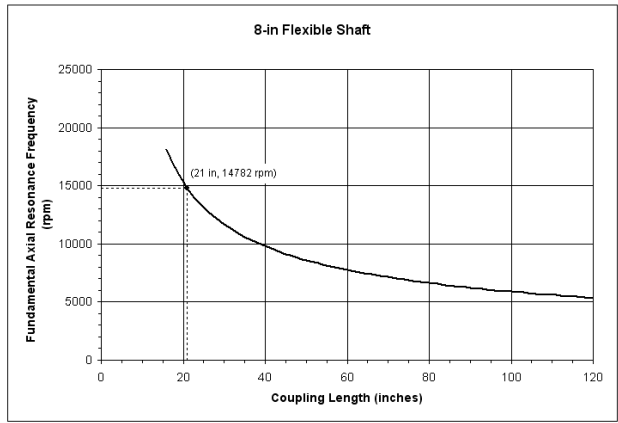
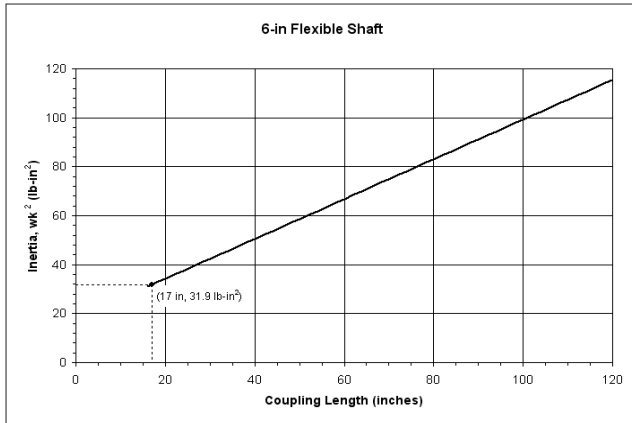
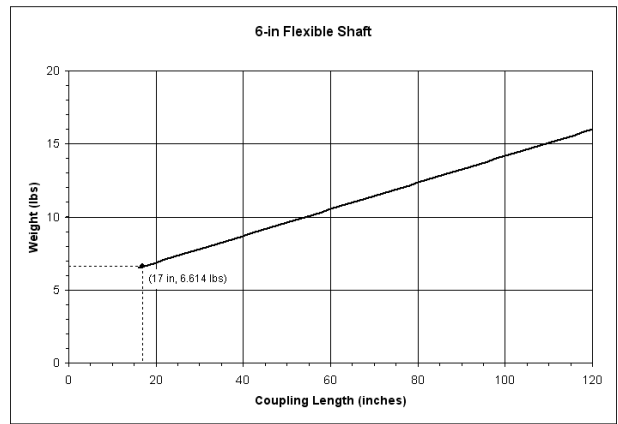
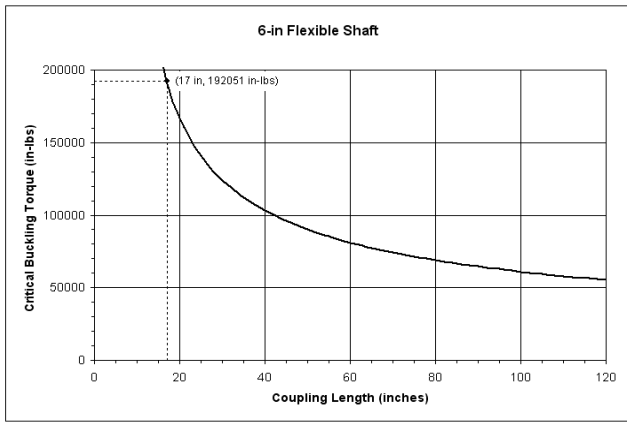


Figure 15 Torque Imposed on a Family of 6_Inch Diameter Hyperbolic Coupling Geometries in Response to 1/2 degree Rotation about the Shaft Axis





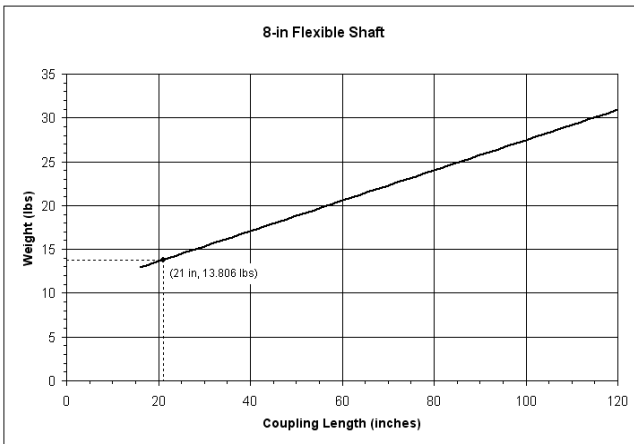
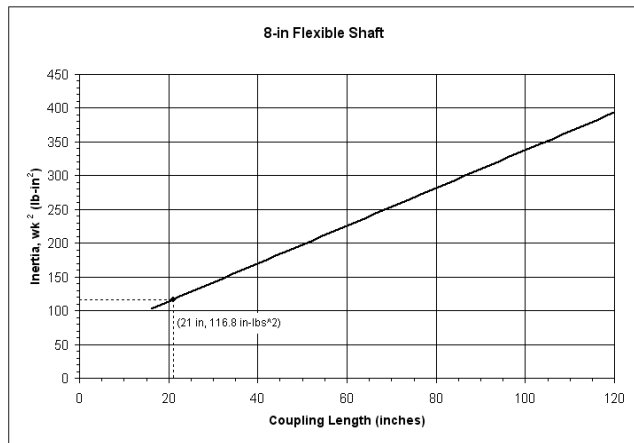


Figure 16 Survey of shaft design parameters

Conclusions

A methodology has been developed by which all-composite, fully integral flexible driveshafts can be designed and produced to take advantage of both part count reduction, and overall weight savings approaching 50% when compared with incumbent assembled titanium flex elements and carbon fiber spacing tubes.

A manufacturing process that provides for precise and repeatable CNC control also uses the perfect geodesic path to maximize torque density. Under imposed axial and bending motions a design space has been identified that minimizes diaphragm bending stresses using hyperbolic geometry just thick enough to avoid torsional buckling of the diaphragm. A case has been made for increased torque and bending motions when shafts are installed with axial pre-tension and operational compression is avoided.

Acknowledgements

Early support for discrete composite flex elements was provided by NAVAIR Pax River, MD. The author extends his appreciation for the collective insight and contributions of the following:

Mr. Ed Evans	Penn State University, Erie
Mr Jim Webb	Cranfield University, UK
DR. Hany Ghoneim	Rochester Inst. Of Technology
Dr. Boris Shoykhet	Rockwell Automation
Mr. Ilan Hoenigsberg	Israeli Aircraft Industries
Mrs. Sonja Clark	Pankl Aerospace
Mr. Robert Schreiber	Pankl Aerospace
Mr. Charlie Kilmain	Bell Helicopter-Textron

Also, thanks are due to Tom McFarland and Ray Brown of Lawrie Technology, Inc. for persisting through over 200 prototype builds over six years as we slowly made sense of this complex project.

References

1 Faust, H.S., Hogan, E.M., Margashahayam, R.N., and Hess, J, 1988, "Development of an integral composite driveshaft and coupling" National Tech. Specialists Meeting on Advanced Rotorcraft Structures